

See discussions, stats, and author profiles for this publication at: <https://www.researchgate.net/publication/51194825>

# Tandem Mass Spectrometry of Uranium and Uranium Oxides in Airborne Particulates

ARTICLE *in* ANALYTICAL CHEMISTRY · JANUARY 1998

Impact Factor: 5.64 · DOI: 10.1021/ac970505g · Source: PubMed

---

CITATIONS

32

---

READS

9

5 AUTHORS, INCLUDING:



Peter T A Reilly

Washington State University

62 PUBLICATIONS 1,115 CITATIONS

SEE PROFILE

# Tandem Mass Spectrometry of Uranium and Uranium Oxides in Airborne Particulates

Rainer A. Gieray, Peter T. A. Reilly, Mo Yang, William B. Whitten,\* and J. Michael Ramsey

Chemical and Analytical Sciences Division, Oak Ridge National Laboratory, P.O. Box 2008, Oak Ridge, Tennessee 37831-6142

**A method for detection of uranium in airborne microparticles in real time has been developed. Positive identification of uranium is achieved by isolating  $\text{UO}^{2+}$  ions and following their reaction with residual oxygen molecules to yield  $\text{UO}_2^+$ .**

The detection of uranium in airborne effluents from nuclear production facilities is of current importance to identify particle emissions from active and inactive plants and to monitor the effectiveness of site remediation efforts.<sup>1</sup> One method that can be used on-line is laser ablation mass spectrometry of individual airborne microparticles.<sup>2</sup> With laser ablation in time-of-flight mass spectrometry, the principal U-containing ions that are observed are atomic  $\text{U}^+$ ,  $m/z$  238, and the two oxide species,  $\text{UO}^+$  and  $\text{UO}_2^+$ , at  $m/z$  256 and 270.<sup>3,4</sup> The  $\text{U}^{2+}$  ion at  $m/z$  119 can be detected at high laser fluence.<sup>4</sup> The  $\text{UO}^+$  ion was used by Stoffels et al.<sup>1</sup> for thermal ionization sector mass spectrometry. In matrixes where there is little isobaric interference, these ions can be formed and detected with high efficiency. However, it has been apparent in various investigations of environmental particles that potential interferences from molecular species with  $m/z$  values distributed throughout the range expected for uranium and its oxides are observed for many particles.<sup>5–7</sup> In the present experiments, where individual airborne particles were analyzed by laser ablation mass spectrometry in an ion trap, reactions of the trapped ions with residual oxygen cause the  $\text{UO}_2^+$  ion to be the major observed species with  $\text{UO}^{2+}$  at  $m/z$  127 also being observed. Our attempts to verify the presence of  $\text{UO}_2^+$  by ion trap collisional activation have been unsuccessful, due presumably to rapid reaction of collisionally produced  $\text{UO}^+$  with neutral species and to the large, 7.8-eV dissociation energy. The purpose of this paper is to report that tandem mass spectrometry of the  $\text{UO}^{2+}$  ion at  $m/z$  127 via ion–molecule reactions with residual oxygen and monitoring of

the associated product ions can be used to verify the presence of uranium in laser ablation mass spectra.

## EXPERIMENT

Airborne microparticles were analyzed by laser ablation mass spectrometry in an ion trap mass spectrometer with a direct atmospheric sampling input, as described by Reilly et al.<sup>8</sup> The instrument was modified so that particle aerodynamic size could be measured along with the mass spectrum.<sup>9</sup> Most of the samples for this investigation were particles formed by evaporating droplets nebulized from a solution. Hospitak disposable nebulizers were used to avoid memory effects. For some measurements, solid microparticles were aerosolized directly by blowing a jet of air across a powdered sample. Microparticles containing trace quantities of uranium were generated by nebulizing an aqueous solution. Solutes used included potassium nitrate and 7-amino-1,3-naphthalenedisulfonic acid (ANDSA). Uranyl nitrate in 5%  $\text{HNO}_3$ , 1000  $\mu\text{g mL}^{-1}$  concentration (ICP standard solution), was added to the solution to attain the desired concentration, ranging from 1 to 1000  $\mu\text{g/g}$  in the dried particles. Salt concentrations in the nebulized solutions were chosen to give dried particles of  $\sim 1\text{-}\mu\text{m}$  diameter. Samples of  $\text{CaF}_2$  crystals containing 500 ppm uranium were also measured for comparison.

Laser ablation of the incoming particles was accomplished with an excimer laser with pulses of  $\sim 10$  ns in duration, 308 nm in wavelength, and 5 mJ in energy, for a fluence of  $\sim 2$  J  $\text{cm}^{-2}$ . Operation of the ion trap to acquire primary and tandem mass spectra of the laser-generated ions has been described by Reilly et al.<sup>8</sup> ICMS software<sup>10</sup> was used to control the mass scans after a particle had been sampled. MS/MS spectra were obtained either after collision-induced dissociation or ion–molecule reactions. As in our previous experiments, the ion capture voltage on the ring electrode, mass selection, and mass scan range were set up initially and the instrument would then operate autonomously, measuring and storing a mass spectrum for each detected particle.

The mass scan rate of the ion trap mass spectrometer was  $\sim 180$   $\mu\text{s amu}^{-1}$ . Therefore, a continuous mass scan between doubly and singly charged uranium ions or oxide ions would require times on the order of 25 ms. The doubly charged ions would have been ejected at the initial part of this interval so ion–

(1) Stoffels, J. J.; Wacker, J. F.; Kelley, J. M.; Bond, L. A.; Kiddy, R. A.; Brauer, F. P. *Appl. Spectrosc.* **1994**, *48*, 1326–1330.

(2) Johnston, M. V.; Wexler, A. S. *Anal. Chem.* **1995**, *67*, 721A–726A.

(3) Sprey, B.; Bochem, H.-P. *Fresenius Z. Anal. Chem.* **1981**, *308*, 239–245.

(4) Reilly, P. T. A.; Gieray, R. A.; Yang, M.; Whitten, W. B.; Ramsey, J. M., unpublished results.

(5) Dotter, R. N.; Smith, C. H.; Young, M. K.; Kelly, P. B.; Jones, D. A.; McCauley, E. M.; Chang, D. P. Y. *Anal. Chem.* **1996**, *68*, 2319–2324.

(6) Hachimi, A.; Krier, G.; Poitevin, E.; Schweigert, M. C.; Peter, S.; Muller, J. F. *J. Environ. Anal. Chem.* **1996**, *62*, 219–230.

(7) Balasamugam, K.; Viswanadham, S. K.; Hercules, D. M. *Talanta* **1989**, *36*, 117–124.

(8) Reilly, P. T. A.; Gieray, R. A.; Yang, M.; Whitten, W. B.; Ramsey, J. M. *Anal. Chem.* **1997**, *69*, 36–39.

(9) Noble, C. A.; Prather, K. A. *Environ. Sci. Technol.* **1996**, *30*, 2667–2680.

(10) Yost, R. A.; et al. ICMS Ion Trap Software Version 2.20.

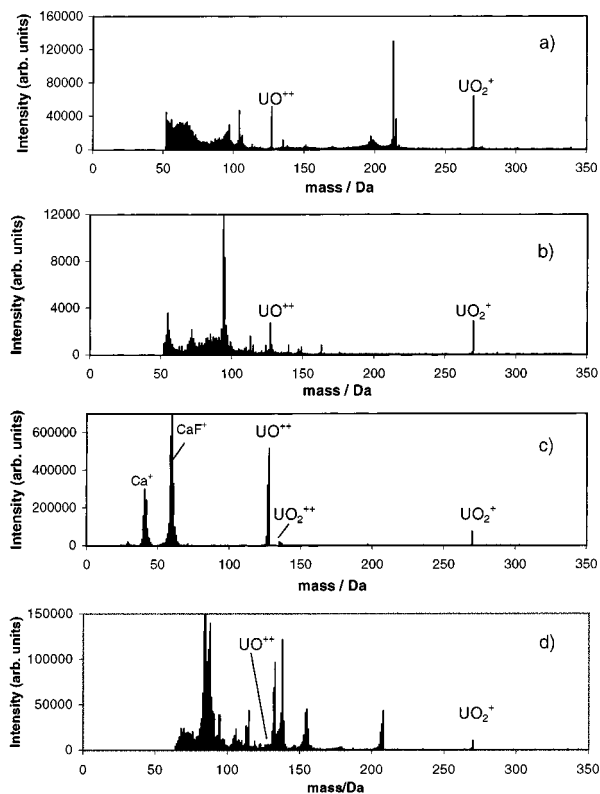


Figure 1. Primary mass spectra of uranium in particles of different substances, averaged over many particles: (a) ANDSA plus 16.8  $\mu\text{g/g}$  U; (b) potassium nitrate plus 1.25 mg/g U; (c) calcium fluoride plus 500  $\mu\text{g/g}$  U; (d) NIST SRM 2710, Montana soil, 25  $\mu\text{g/g}$  U.

molecule reactions involving these ions would be negligible after this time. Already-formed intermediate species could continue to react until they were ejected, however, resulting in a lower measured population for these ions than would be obtained under steady-state conditions. Accordingly, mass scans after isolation were sometimes started close to the  $m/z$  value of a target species to analyze for transient species with high reaction rates. Most of the measurements were made with the residual air partial pressure of  $4 \times 10^{-5}$  Torr, corresponding to an oxygen concentration of  $2.8 \times 10^{11} \text{ cm}^{-3}$ . In some experiments, additional air or water vapor was added to the trap to influence the reaction rates.

## RESULTS AND DISCUSSION

This section is presented in two parts. First, primary mass spectra are used to identify uranium ion reactants, intermediates, and products as well as measure their decay rates. In the second part, MS/MS measurements are used to determine the reaction mechanism and demonstrate a sensitive and positive method of identification of uranium in complex matrixes that should prove useful in environmental analysis.

**Primary Mass Spectra.** Primary mass spectra of uranium in several arbitrarily selected matrixes, ANDSA, potassium nitrate, and calcium fluoride, are shown in Figure 1a–c, respectively. In addition, the average mass spectrum of particles from NIST Standard Reference Material 2710, Montana soil, is shown in Figure 1d. The uranium concentration for this material is reported to be 25  $\mu\text{g/g}$  (uncertified). Two prominent masses observed in these matrixes were attributed to uranium:  $\text{UO}_2^+$  at  $m/z$  270 and

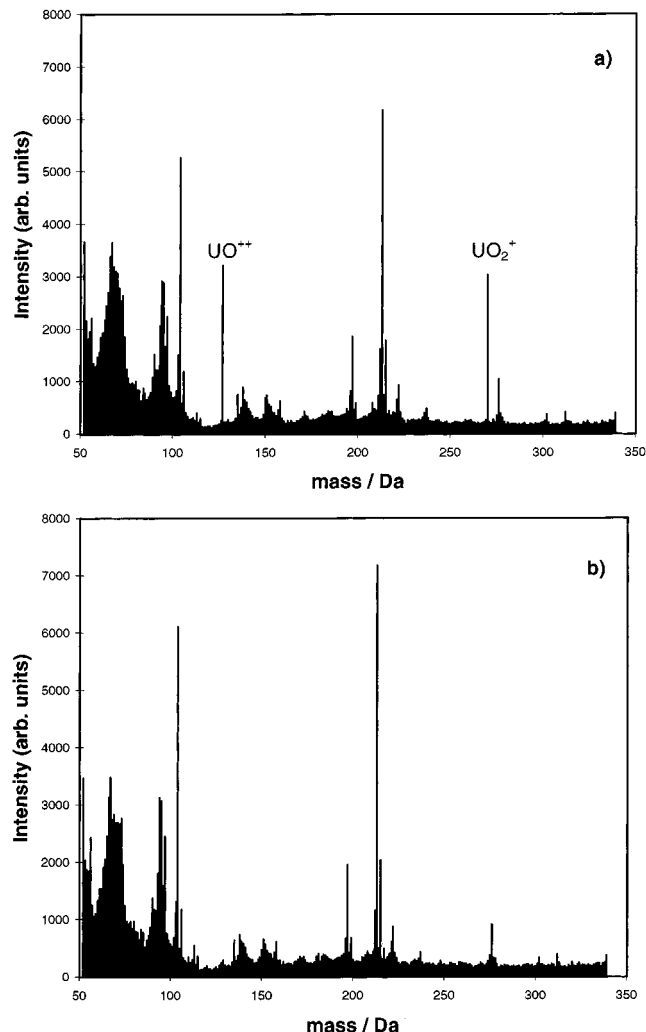


Figure 2. Primary mass spectra of uranium in ANDSA, average of several hundred particles with mean diameter of 0.7  $\mu\text{m}$ : (a) ANDSA plus 1.8  $\mu\text{g/g}$  U as uranyl nitrate; (b) blank.

$\text{UO}^{2+}$  at  $m/z$  127. Minor ions at  $m/z$  287,  $\text{UO}_2\text{OH}^+$ , and  $m/z$  135,  $\text{UO}_2^{2+}$ , were sometimes observed in the primary spectrum. The uranium contributions to the mass spectra were qualitatively similar for all matrixes studied here. However, the sensitivity or detection limit depended strongly of the matrix, being  $\sim 3$  orders of magnitude worse for potassium nitrate than for ANDSA particles.

To explore the limit of detection, measurements were made on ANDSA particles at lower uranium concentrations as well as blank determinations. In Figure 2a, we show the mass spectrum obtained from several hundred particles of ANDSA with 1.8  $\mu\text{g/g}$  uranyl nitrate added, measured individually with 5-mJ pulses at 308 nm but averaged for the plot. Only particles between 0.5 and 1.0  $\mu\text{m}$  in diameter were included. The geometric diameter was calculated from the measured aerodynamic diameter with the assumption that the particles were spherical with a density of  $1.5 \text{ g cm}^{-3}$ . The mean diameter of the particles was 0.7  $\mu\text{m}$  with a standard deviation of 0.15  $\mu\text{m}$ . The mass of a 0.7- $\mu\text{m}$  particle is 0.3 pg so the average detected uranium for this size particle was less than 0.6 ag. A similar measurement with no uranium added is shown in Figure 2b. The ultimate uranium detection limit is thus in the subattogram range in a favorable matrix.

Table 1. Ion–Molecule Reaction Decay Constants, at  $4 \times 10^{-5}$  Torr Air Pressure

ion	decay const ( $s^{-1}$ )	time const (ms)	ion	decay const ( $s^{-1}$ )	time const (ms)
$U^{2+}$	330	3.0	$UO^+$	260	3.8
$UO_2^{2+}$	160	6.2	$UO_2^+$	8	120
$U^+$	220	4.6			

The various uranium ions could have been produced either by the laser ablation/ionization event or by ion–molecule reactions with the background gas since not all of the ambient air was removed and the ions were stored for tens of milliseconds before they were ejected. TOF spectra from uranium carrying algae<sup>3</sup> and uranium-containing ANDSA particles<sup>4</sup> were used to determine which ions were created during the ablation/ionization event ( $t = 0$  ions). Ions ablated from particles examined using time-of-flight mass spectrometry would not have enough time (less than a few microseconds) to react with background gases before their extraction into the flight tube; therefore, uranium-containing ions in the TOF spectra were created during and just after the laser pulse. The predominant ions in the TOF spectra were  $U^{2+}$ ,<sup>4</sup>  $U^+$ ,  $UO^+$ , and  $UO_2^+$ <sup>3,4</sup> (A mass at  $m/z$  119,  $U^{2+}$ , was present but not identified in the algae spectra). The  $t = 0$  ions in the ion trap should have the same composition and distribution as those observed in the TOF spectra. Presumably, the other ionic species observed in the ion trap spectra,  $UO_2^+$ ,  $UO_2^{2+}$ , and the occasionally seen  $UO_2OH^+$ , were created in the ion trap by reaction of  $t = 0$  ions with the background gas. (See first row in Figure 4.)

While the  $U^{2+}$ ,  $U^+$ , and  $UO^+$  ions could not be detected in a normal ion trap scan, it was possible to observe them and measure their decay when the intrinsic delays were minimized by starting the mass scan close to the ion of interest. To measure the decay of particular ions in the ion trap, the trapping potential was set so that the masses below the mass of interest were ejected. A delay between the laser pulse and the start of the scan was then varied and intensity of the ion was observed. Decay rates measured at the residual air partial pressure of  $4 \times 10^{-5}$  Torr are presented in Table 1. The rapid decay rates show that under normal scanning conditions where a wide mass range was scanned, the  $U^{2+}$ ,  $U^+$ , and  $UO^+$  ions created by the laser pulse would not be observable. When the RF trapping potential was set so that masses below  $m/z$  120 were ejected from the trap, the disappearance of the  $UO_2^+$  and  $UO_2^{2+}$  ions confirmed that  $U^{2+}$ ,  $m/z$  119, was the source of the  $UO_2^+$  and  $UO_2^{2+}$ . This was not surprising since  $U^{2+}$  is the only doubly charged ion created by the laser pulse.  $UO_2^+$  was only observed to decay when the trap depth was small enough to permit collisional detrapping. The most notable feature of Table 1 is the relatively slow decay rate of  $UO_2^+$ . This slow decay together with the stability of  $UO_2^+$  account for the prominence of the two ions in the primary ion trap mass spectra. It is also apparent that the end product of the decay of the  $t = 0$  uranium ions is eventually  $UO_2^+$ .

#### MS/MS SPECTRA

Using the methods of ion trap tandem mass spectrometry, we were able to isolate the ions at  $m/z$  127 and subsequently analyze the product ions formed by reaction of the precursor with the

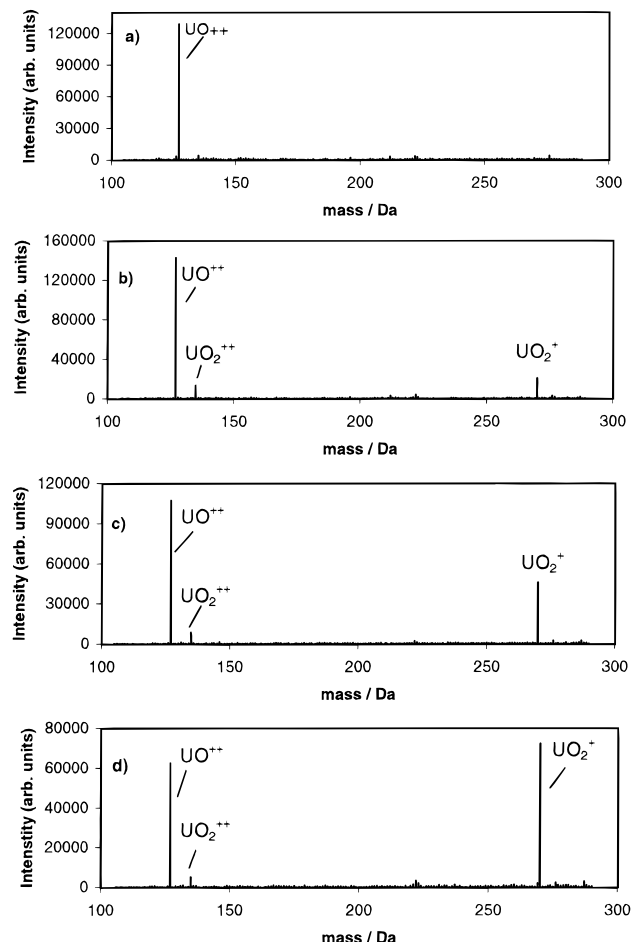
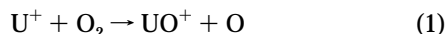


Figure 3. MS/MS experiments showing increase of  $UO_2^+$  with time from isolated  $UO_2^+$  ions. The concurrent growth of  $O_2^+$  is not shown here because ions with  $m/z$  below 100 were not trapped in these scans. The times from the laser pulse until the appearance of ions at  $m/z$  127 for the four scans were, from top to bottom, 5.7, 60.7, 145.7, and 255.7 ms.

background gas. In Figure 3, we show a sequence of measurements with varying time delays between isolation of  $m/z$  127 and the scan of the reaction product spectrum. The growth of  $UO_2^+$  with time is evident. The ions at  $m/z$  127 react with the background  $O_2$  to eventually yield  $UO_2^+$  at  $m/z$  270 and  $O_2^+$  at  $m/z$  32 (not shown in Figure 3). Intermediate species in this reaction, particularly  $UO_2^{2+}$  and  $UO^+$ , were sought by starting the mass scan just below the mass of interest. Only  $UO_2^{2+}$  was detected in these experiments. A small concentration of  $UO_2^{2+}$  can be seen at  $m/z$  135 in the delayed scans of Figure 3.

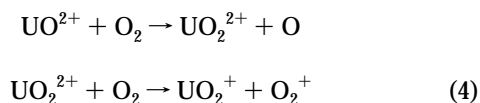
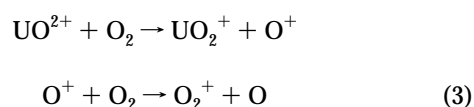
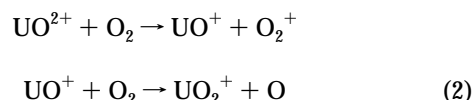
In the present experiment, where ambient air was admitted into the vacuum system along with the airborne particles being analyzed, there was only partial control of the composition of the molecular background in the ion trap. We therefore must speculate to some degree on the background reactants. Since all of the products and intermediates contain oxygen, only oxygen-containing reactants need be considered.  $O_2$  and  $H_2O$  seem the most likely candidates. MS/MS experiments on  $m/z$  127 while water vapor was admitted to the vacuum chamber showed production of significant amounts of  $UO_2OH^+$  as well as  $UO_2^+$ . Since  $UO_2OH^+$  was rarely detected in our experiments when water was not deliberately added, we suggest that  $O_2$  is the primary

background gas reagent. This is further confirmed by the measured decay rate for  $\text{U}^+$ . If one assumes this decay is due to reaction with  $\text{O}_2$  exclusively according to the following reaction,



and that 20% of the background air is composed of  $\text{O}_2$ , then the rate constant for reaction 1 is  $8 \times 10^{-10} \text{ cm}^3 \text{ s}^{-1}$ . This agrees very well with the rate constant of  $8.5 \times 10^{-10} \text{ cm}^3 \text{ s}^{-1}$  given by Johnsen and Biondi<sup>11</sup> for the same reaction and helps to confirm  $\text{O}_2$  as the primary reactant in the background gas.

The following sets of reactions represent the three most plausible paths from  $\text{UO}^{2+}$  to  $\text{UO}_2^+$  in the MS/MS experiments of  $m/z$  127:



Pathway 2 can be rejected as being dominant since no  $\text{UO}^+$  intermediate was observed in the MS/MS experiment, yet this species was readily observable immediately after the laser pulse. An upper limit for the decay rate for the first reaction in pathway 2 is  $0.9 \text{ s}^{-1}$ , based on our estimated signal-to-noise ratio and the measured decay rates of  $\text{UO}^{2+}$  and  $\text{UO}^+$ . This is 1 order of magnitude smaller than the measured decay rate of  $\text{UO}^{2+}$ . Pathway 3 may also be rejected as the dominant path since setting the trapping potential so that  $m/z$  16,  $\text{O}^+$ , was immediately ejected from the trap had no observable effect on the rate of production of  $\text{O}_2^+$ . To confirm that (4) must be the principal reaction pathway, an MS/MS experiment on  $m/z$  127 was carried out with resonant ejection of  $m/z$  135,  $\text{UO}_2^{2+}$ . The  $\text{UO}_2^+$  product was strongly suppressed in this experiment. MS/MS experiments on  $m/z$  135 showing production of  $\text{O}_2^+$  and  $\text{UO}_2^+$  were further confirmation.

A reaction scheme that is consistent with our experimental observations is shown in Figure 4. The four species shown on the top line are generated during the laser ablation/ionization event, either by the laser pulse or subsequent collisions as the plume expands. Following the ablation, the stored ions react with residual oxygen, with  $\text{U}^{2+}$  converting rapidly to  $\text{UO}^{2+}$ , and with  $\text{U}^+$  and  $\text{UO}^+$  converting to  $\text{UO}_2^+$  with a high enough rate that

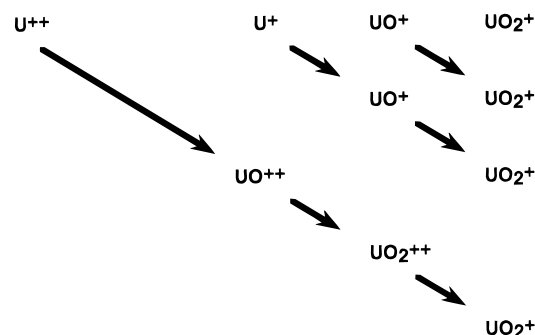


Figure 4. Reaction pathways in the ion trap MS/MS analysis of uranium. Ions in top line formed during laser ablation; ions below formed by reactions of stored ions with residual  $\text{O}_2$ .

they are not detectable in the conventional ion trap mass scan. The relatively inert  $\text{UO}_2^{2+}$  slowly converts to  $\text{UO}_2^+$  in a two-step reaction with  $\text{UO}_2^{2+}$  as an intermediate.

## CONCLUSIONS

We have shown that uranium can be detected at the attogram level or better in microparticle samples by laser ablation ion trap mass spectrometry, with  $\text{UO}_2^+$  being monitored. However, the detection efficiency strongly depends on the particle matrix. The method may be useful as an on-line monitoring system to determine the fraction of uranium-containing particles in the atmospheric environment. Together with other information from the mass spectra, it might be possible to identify the origin of the particles. If isobaric interferences are encountered, positive identification of uranium can be assured by following the ion-molecule reaction of isolated  $\text{UO}_2^{2+}$  ions with residual oxygen molecules in the ion trap to yield  $\text{UO}_2^+$  ions. In our experiments, approximately the same level of  $\text{UO}^{2+}$  as  $\text{UO}_2^+$  was observed in the primary mass spectra, so comparable detection limits should be achievable after isolation of  $\text{UO}^{2+}$  in the MS/MS determination. It is possible to alter the concentration of reagent molecules in the trap to vary the rates of the reactions and reaction products to further enhance the analytical power of the method. However, the kinetics of the ion-molecule reactions that were observed to take place in the trap were favorable for tandem mass analysis with no alteration in measurement conditions.

## ACKNOWLEDGMENT

This research was sponsored by the U.S. Department of Energy, Office of Research and Development and Office of Basic Energy Sciences. Oak Ridge National Laboratory is managed by Lockheed Martin Energy Research Corp., for the U.S. Department of Energy under Contract DE-AC05-96OR22464.

Received for review May 15, 1997. Accepted October 10, 1997.<sup>®</sup>

AC970505G

(11) Johnsen, R.; Biondi, M. A. *J. Chem. Phys.* **1972**, *57*, 1975–1979.

<sup>®</sup> Abstract published in *Advance ACS Abstracts*, December 1, 1997.